

**UCC Library and UCC researchers have made this item openly available.
 Please [let us know](#) how this has helped you. Thanks!**

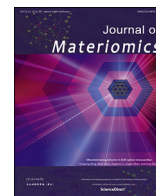
Title	Long-term stability of transparent n/p ZnO homojunctions grown by rf-sputtering at room-temperature
Author(s)	Kampylafka, V.; Kostopoulos, A.; Modreanu, Mircea; Schmidt, Michael; Gagaoudakis, E.; Tsagaraki, K.; Kontomitrou, V.; Konstantinidis, G.; Deligeorgis, G.; Kiriakidis, G.; Aperathitis, E.
Publication date	2019-02-13
Original citation	Kampylafka, V., Kostopoulos, A., Modreanu, M., Schmidt, M., Gagaoudakis, E., Tsagaraki, K., Kontomitrou, V., Konstantinidis, G., Deligeorgis, G., Kiriakidis, G. and Aperathitis, E., 2019. Long-term stability of transparent n/p ZnO homojunctions grown by rf-sputtering at room-temperature. Journal of Materiomics. (8pp). DOI: 10.1016/j.jmat.2019.02.006
Type of publication	Article (peer-reviewed)
Link to publisher's version	http://www.sciencedirect.com/science/article/pii/S2352847818301898 http://dx.doi.org/10.1016/j.jmat.2019.02.006 Access to the full text of the published version may require a subscription.
Rights	© 2019 The Chinese Ceramic Society. Production and hosting by Elsevier B.V https://creativecommons.org/licenses/by-nc-nd/4.0/
Item downloaded from	http://hdl.handle.net/10468/9185

Downloaded on 2020-06-06T01:17:01Z



Contents lists available at ScienceDirect

Journal of Materiomics

journal homepage: www.journals.elsevier.com/journal-of-materiomics/

Long-term stability of transparent n/p ZnO homojunctions grown by rf-sputtering at room-temperature

V. Kampylafka^a, A. Kostopoulos^a, M. Modreanu^b, M. Schmidt^b, E. Gagaoudakis^{c,d},
K. Tsagaraki^a, V. Kontomitrou^a, G. Konstantinidis^a, G. Deligeorgis^a, G. Kiriakidis^{c,d},
E. Aperathitis^{a,*}

^a Microelectronics Research Group, Institute of Electronic Structure and Laser, Foundation for Research and Technology—FORTH-Hellas, P.O. Box 1385, Heraklion, 70013, Crete, Greece

^b Tyndall National Institute-University College Cork, Lee Maltings, Dyke Parade, Cork, Ireland

^c Physics Department, University of Crete, P.O. Box 2208, 71003, Heraklion, Crete, Greece

^d Transparent Conductive Materials & Devices Group, Institute of Electronic Structure & Laser, Foundation for Research and Technology FORTH-Hellas, P.O. Box 1385, Heraklion, 70013, Crete, Greece

ARTICLE INFO

Article history:

Received 23 November 2018

Received in revised form

22 January 2019

Accepted 12 February 2019

Available online xxx

Keywords:

ZnO homojunction

p-type ZnO

Single step sputtering

Stability

Patterned substrate

ABSTRACT

ZnO-based n/p homojunctions were fabricated by sputtering from a single zinc nitride target at room temperature on metal or ITO-coated glass and Si substrates. A multi-target rf-sputtering system was used for the growth of all oxide films as multilayers in a single growth run without breaking the vacuum in the growth chamber. The nitrogen-containing films (less than 1.5 at.% of nitrogen) were n-type ZnO when deposited in oxygen-deficient Ar plasma (10% O₂) and p-type ZnO when deposited in oxygen-rich Ar plasma (50% O₂). The all-oxide homojunction ITO/n-ZnO/p-ZnO/ITO/glass was fabricated in a single deposition run and exhibited visible transparency in the range of 75–85%. The n/p ZnO homojunctions, having metallic contacts, formed on conventionally processed substrates showed a fairly unstable behavior concerning the current-voltage characteristics. However, the same homojunctions formed on Si₃N₄-patterned substrates and stored in atmosphere for a period of five months were stable exhibiting a turn-on voltage of around 1.5 V. The realization of a room temperature sputtered transparent and stable ZnO homojunction paves the way to the realization of all-oxide transparent optoelectronic devices.

© 2019 The Chinese Ceramic Society. Production and hosting by Elsevier B.V. This is an open access article under the CC BY-NC-ND license (<http://creativecommons.org/licenses/by-nc-nd/4.0/>).

1. Introduction

Over the last decade the rapid development in optoelectronic devices like solar cells, sensors and light emitting diodes, combined with transparency and flexibility, has lead to applications in a variety of fields spanning from consumable portable and wearable electronic products [1,2], energy and environment [3,4] to bio- and nano-technology materials for human health [5]. Main requirements for these devices have been the realization of the vital component of solid state electronics namely the n/p junction, a reliable operation, the low temperature fabrication processes and the high performance at low manufacturing cost.

Zinc oxide (ZnO) is an extensively studied material for

optoelectronic applications because it combines attractive physical properties (optical transparency, high exciton binding energy, high piezoelectricity and a low thermal expansion coefficient) with abundance and no hazardous or toxic characteristics. Nonetheless, ZnO is an intrinsically n-type material caused by excess Zn and oxygen deficient structure. Due to the inherent difficulty to form reliable and controllably stable p-type material (arising from self-compensation effects, deep acceptor levels and low solubility of acceptors) the use of ZnO has been restricted only either as a passive transparent conductive layer or as active n-type material in n/p heterostructures where the p-type element may be a different material such as GaN, Si, NiO, SiC, etc [6,7]. However, crystallographic mismatch, lattice misalignment and energy band discontinuities at the n-p interfaces of such heterostructures generally lead to electrical or optical active defects (traps) which degrade the output characteristics of the resulting device. To eliminate such drawbacks, including fabrication costs issues, attempts have been

* Corresponding author.

E-mail address: eper@physics.uoc.gr (E. Aperathitis).

Peer review under responsibility of The Chinese Ceramic Society.

<https://doi.org/10.1016/j.jmat.2019.02.006>

2352-8478/© 2019 The Chinese Ceramic Society. Production and hosting by Elsevier B.V. This is an open access article under the CC BY-NC-ND license (<http://creativecommons.org/licenses/by-nc-nd/4.0/>).

made towards a stable and controllable p-type ZnO for the fabrication of n/p ZnO homojunctions. Along these lines, p-type doping engineering has been reported for creating acceptor dopants in ZnO, such as excess oxygen in the film during deposition [8], single doping from group-I (Ag, Li, Na, K) or group-V (N, P, As, Sb) elements and dual doping (P–N, Li–N, Ag–N, etc.) or co-doping with donor and acceptor (Ag–N, Al–N, In–N, etc.) [7]. Nonetheless, due to similarities of electronegativity and ionic radius between nitrogen and oxygen, nitrogen is the most attractive and commonly used dopant for p-type ZnO. Thus, n/p or p/n ZnO homojunctions, either as thin films or as nano-rods, have been developed by sputtering [8–12], laser assisted molecular beam epitaxy [13], chemical vapour deposition [14,15], pulsed laser deposition [16–18], sol gel [19]), spray pyrolysis [20–23] and atomic layer deposition [24]. The majority of these techniques utilize high temperatures ($>300^\circ\text{C}$) either during deposition to improve the quality of the structure or/and after deposition to improve the ohmic contacts or activate the n/p ZnO homojunction. This, however, creates major technical limitations if these devices are to be applied for emerging portable, bendable or wearable applications. Until today fabrication of n/p ZnO at room temperature has been realized only by plasma containing deposition techniques, namely sputtering [25] or plasma assisted molecular beam epitaxy [26]. Irrespective of the method of fabrication, a number of n/p ZnO homojunctions issues concerning the long term stability and the rectification properties of the homodiode have been reported and attempts have been made to overcome them. For example, deterioration of the junction due to contamination from the ambient atmosphere has been investigated by fabricating the diode in both p/n and n/p configurations [24], unstable defects were eliminated by modifying deposition conditions [18] whereas inter-diffusion of nitrogen at the interface [14] has been tackled by inserting an ultrathin Al_2O_3 layer at the n-p interface [24].

In a previous investigation we had shown that nitrogen-containing ZnO layers, of both n- and p-type conductivity, could be fabricated at room temperature from a single zinc nitride sputtering target by adjusting the oxygen content in the Ar plasma during deposition [27]. In this way, it was possible to realize an n-ZnN/p-ZnO heterostructure by fabricating all layers in a single growth run without chamber vent. In this work we present the fabrication of an n/p ZnO homojunction structure from a single sputtering target at room temperature on unpatterned and Si_3N_4 -patterned substrates along with an investigation of the long term behavior. The realization of an n/p ZnO on a patterned substrate at room temperature is a novel approach for fabricating all-oxide transparent n/p ZnO homojunctions with improved stability for transparent as well as on-chip integration applications.

2. Experimental Details

2.1. Thin films deposition

The thin films used in this investigation, zinc oxide (ZnO) and indium tin oxide (ITO), were deposited by employing the rf (radio frequency) sputtering technique using a multi-target Nordiko NS2500 system equipped with rotatable substrate holder. The multilayer structures reported in this paper were deposited in a single deposition run without venting the chamber, thus eliminating possible contamination of the layers' interface. The mixture of the gases (i.e. Ar and O_2) was controlled by varying their flows, through calibrated mass flow controllers, so that the total pressure in the chamber was kept constant. Prior to each deposition run, the sputtering chamber was pumped down to a base pressure better than 1×10^{-6} mbar (1×10^{-4} Pa). The target-substrate distance was 10 cm and UV-grade fused silica and pieces of Si (100) wafer were

used as substrates. The native oxide on the Si substrates was removed in diluted HF solution and all substrates were cleaned in organic solvents (acetone and 2-propanol), thoroughly rinsed in 18 M Ω de-ionized water and blow-dried using N_2 flow.

The zinc oxide thin films were deposited from a 6-inch diameter zinc nitride target. The rf-power used was 100 W, the total pressure was 5 mTorr (0.67 Pa) and 10% O_2 or 50% O_2 in Ar plasma was used for growing n-type ZnO and p-type ZnO films, respectively. Details of the deposition conditions of ZnO films can be found elsewhere [27]. Before each ZnO deposition run the target was pre-cleaned initially in Ar plasma for 10 min followed by N_2 plasma for 60 min in an attempt to remove any possible contaminants for the surface of the target, keep its stoichiometry and bring it in equilibrium conditions.

Indium tin oxide (ITO) was used in order to test the transparency of the ZnO homojunctions in the ITO/n-ZnO/p-ZnO/ITO/glass configuration. The ITO thin films were deposited from an indium-tin-oxide target (80% In_2O_3 –20% SnO_2) in pure Ar, at 5 mTorr (0.67 Pa) pressure and 300 W rf-power. The ITO-coated substrates were annealed in a Rapid Thermal Annealing system (JIPLEC FAV4) for 1 min at 400°C in N_2 atmosphere (450 sccm flow rate) in order to improve the electrical and structural properties of the ITO coating prior the ZnO deposition [28]. The nominal thickness of the ZnO and ITO thin films was around 170 nm unless otherwise indicated.

2.2. ZnO homojunction fabrication

The substrates used for the fabrication of ZnO homojunctions were ITO-coated or Ag/Au-coated glass and Si pieces. The latter metallization, deposited by electron beam evaporation, was used as the ohmic contact to the p-ZnO layer which would be the first layer to be sputter-deposited for the formation of the diode. By exploiting the fact that the ZnO layers of the diode could be formed on unintentionally heated substrates, the sputtering chamber was loaded with the above mentioned substrates which had been patterned with photoresist, having dot geometry with diameter of 700 μm , employing standard optical lithography and lift-off techniques. In addition, the dot geometry patterning was also made on Si_3N_4 -coated substrates. For this case, the formation of the dot geometry was transferred from Si_3N_4 down to the substrate by employing reactive ion etching (RIE). After the p-ZnO and n-ZnO layers deposition, as described above, the samples were removed from the sputtering chamber and the top ohmic contact (Ti/Au) for the n-ZnO was formed by electron beam evaporation followed by lift-off. Alternatively, after the ZnO depositions and without venting the chamber, the sample holder was moved over the ITO target for the deposition of the ITO layer which was followed by the lift-off procedure. In this way, two different diode configurations could be formed in the same growth run, one on conventional substrate and another one on Si_3N_4 -patterned substrates. The cross-sectional schematic representations of the diode configurations can be seen in Fig. 1 where the numbering of the layers gives also the sequence of the processing steps used for the fabrication of the diode. The conventional n/p ZnO diode configuration which was unprotected from the ambient atmosphere is presented in Fig. 1(a), whereas the Si_3N_4 -protected n/p ZnO configuration which, throughout its fabrication, was not exposed to the ambient is seen in Fig. 1(b). The patterned Si_3N_4 layer, which played the role of protective layer for the ZnO homojunction, was formed by Plasma Enhanced Chemical Vapour Deposition (PECVD – Vacutec 1250) in $\text{SiH}_4\text{:NH}_3\text{:N}_2$ plasma at 300°C , had a thickness of around 350 nm and its etching was made in a RIE system (Vacutec 1250) in fluorine containing plasma.

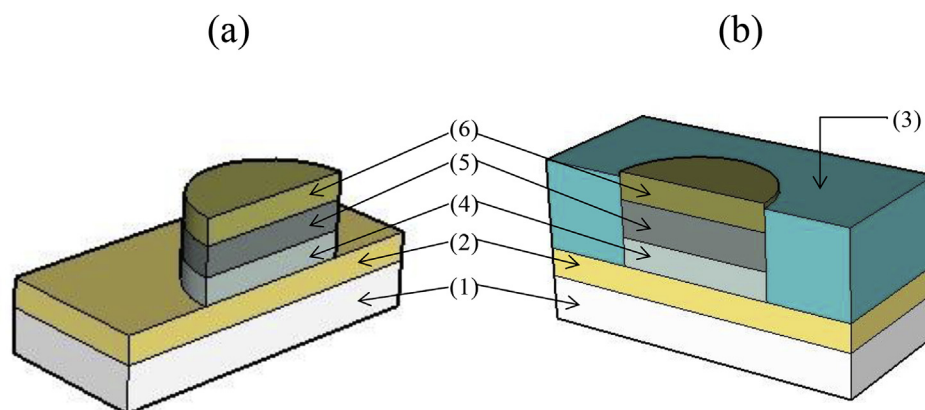


Fig. 1. Schematic representation of n/p ZnO homojunctions on (a) conventional non-patterned substrate and (b) Si_3N_4 -patterned substrate. 1: substrate (glass or Si), 2: bottom contact (metal or ITO), 3: Si_3N_4 , 4: p-ZnO, 5: n-ZnO, 6: top contact (metal or ITO).

2.3. Thin films and device characterization

The structural properties of the films were examined by X-ray diffraction (XRD) and Transmission Electron Microscopy (TEM). XRD measurements were performed using a Rigaku D-max 2000 system, with $\text{Cu K}\alpha 1$ radiation ($\lambda = 1.5405 \text{ \AA}$). The films were scanned in a Bragg-Brentano configuration (θ - 2θ) from 30° to 90° . The surface or the cross-sectional morphologies of the layers were investigated by Field-Emission Scanning Electron Microscope (FE-SEM, Jeol 7000F), operating at 15 keV whereas high resolution cross-sectional Transmission Electron Microscopy (XTEM) imaging was carried out using a JEOL 2100 HRTEM operated at 200 kV in Bright Field (BF) mode and Selective Area Electron Diffraction (SAED) mode using a Gatan Double Tilt holder. The XTEM analysis was made on samples prepared by the Focus Ion Beam technique. The cross-section of the samples was obtained by employing FEI's Dual Beam Helios Nanolab 600i system using Ga ion beam and two layers of protective material were used, namely electron beam Pt and ion beam C. The lamellas were thinned and polished at 30 kV & 100 pA and 5 kV & 47 pA, respectively. Atomic force microscopy (AFM) measurements were performed in order to examine the surface morphology and roughness of the films. A Digital Instrument-Multimode system was employed, with maximum scanning area $100 \mu\text{m} \times 100 \mu\text{m} \times 5.6 \mu\text{m}$, working in the Tapping Mode using Si-sharp tips (radius of curvature 10–15 nm).

The transport properties of the films (resistivity, carrier concentration and Hall mobility) were determined by Hall-effect measurements using the four-probe Van der Pauw technique and the optical properties of the films were examined by recording the transmittance in the UV–Vis–NIR spectrum (Perkin Elmer Lambda 950 spectrophotometer). The transmittance (T) values were used to get an estimation of the optical direct band gap, E_g , of the films through the standard relations $T = \exp(-\alpha d)$, $(\alpha h\nu)^2 = A(h\nu - E_g)$ and the Tauc plot, where α is the absorption coefficient, d is the thickness, h is the Planck's constant and ν is the photon's frequency. All measurements were performed on as-prepared films unless it is stated otherwise and the thickness was determined by using a stylus profilometer (Veeco Dektak 150). The current–voltage (I – V) characteristics of the homodiodes were recorded using a programmable curve tracer (Sony, Tektronix 370).

3. Results and discussion

3.1. Thin films properties

In previous experiments [27,29] it had been shown that films

sputtered from a zinc nitride target in plasma containing a mixture of Ar-O_2 gases could produce n-ZnO films in oxygen-deficient plasma (less than 30% O_2) and p-ZnO in oxygen-rich plasma (more than 40% O_2). Even though the existence of nitrogen in the films could not be detected unambiguously by EDX since its signal was at the detection limit of the system, the n-type conduction (oxygen-deficient plasma) was attributed to donors formed by interstitial zinc and oxygen vacancies, whereas the p-type conduction (oxygen-rich plasma) was due to acceptors formed by zinc vacancies, oxygen interstitial and N-on-O substitutions [6,27,30–32].

The structural properties of the individual n-ZnO and p-ZnO layers which constituted the n/p ZnO homojunction are seen in Fig. 2(a) where the XRD patterns of the films deposited in 10% O_2 and 50% O_2 in Ar plasma are depicted. Both films had the hexagonal wurtzite structure of ZnO with the (002) diffraction peaks located at 34.03° and 34.14° for the films made in low oxygen plasma (10% O_2) and rich oxygen plasma (50% O_2), respectively. The lower diffraction angle of (002) ZnO peaks than that given by the Joint Committee of Powder Diffraction System (JCPDS) card 36–1451 (34.42°) can be attributed to the low temperature fabrication of the films and the associated poor crystallinity of the films [33]. Furthermore, the difference in the (002) diffraction angle between the two films can be attributed to the built-in stress in the structure of the films due to the existence of nitrogen and the different amounts of oxygen in the Zn–O structures, and the differences on the atomic radius of N (0.56 Å) with those of O (0.48 Å) and Zn (1.42 Å) [10–12,29]. The transmittance of the films is presented in Fig. 2(b). Both films have a transparency of ~80–90% in the visible region of the spectrum. The energy band gap of the films, extracted from Tauc plot, was 3.31 eV for the film deposited in 10% O_2 in plasma and 3.35 eV for the 50% O_2 film, indicating an increase of the optical band gap with the O concentration in the layers. The increased transmittance below the absorption edge seen in Fig. 2(b) is a feature generally observed either for undoped or doped ZnO films [33–35]. Table 1 presents the electrical properties of the N-doped ZnO films where it is seen that oxygen-rich plasma (50% O_2) leads to p-type ZnO films but with lower carrier concentration and mobility and higher resistivity than those of n-ZnO films grown in an oxygen-deficient plasma (10% O_2).

The n-type ITO films were used either as transparent and conductive coatings on the substrates and/or as cap-protective layer for the ZnO homojunction. Since it is well established that the properties of any polycrystalline thin film can be improved by post-deposition annealing, ITO-coated substrates had been annealed prior to any further use so to improve their properties [28] whereas

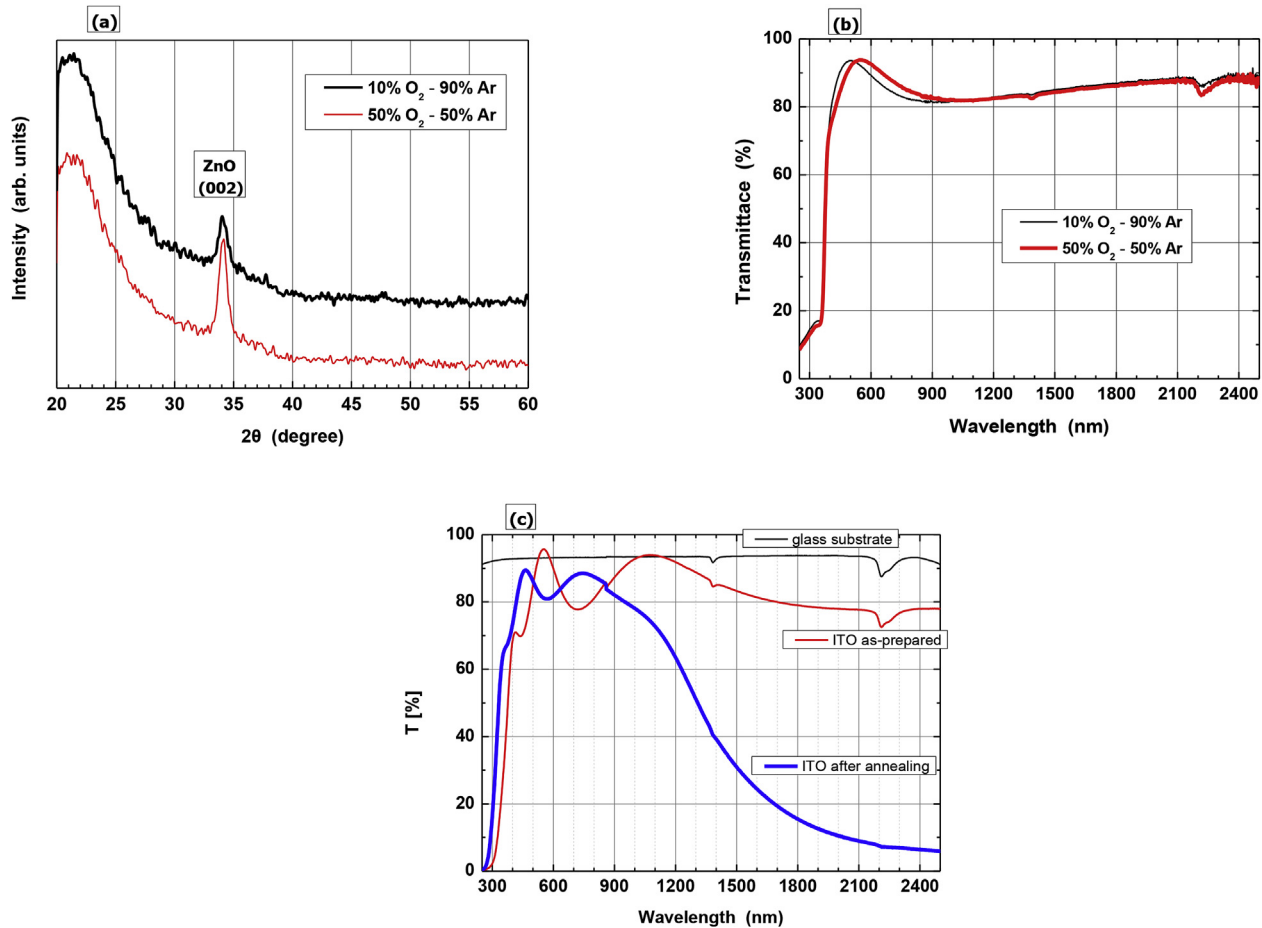


Fig. 2. XRD spectra (a) and transmittance spectra (b) of ZnO films deposited on glass substrates in Ar plasma containing 10% and 50% O₂. (c) Transmittance spectra of the ITO films after deposition and after thermal treatment deposited on glass substrates in Ar plasma. The transmittance of the glass substrate is also shown.

Table 1
Electrical properties of rf sputtered ZnO:N and ITO films on room temperature glass substrates.

Thin film layers (plasma conditions)	Treatment	Sheet Resistance ($\Omega/\text{sq.}$)	Resistivity ($\Omega\cdot\text{cm}$)	Carrier Concentration (cm^{-3})	Mobility (cm^2/Vs)	Type
ZnO:N (10% O ₂ -90% Ar)	As-prepared	9.7×10^4	3.6×10^0	-1.6×10^{18}	7.8×10^0	n
ZnO:N (50% O ₂ -50% Ar)	As-prepared	6.8×10^5	3.2×10^1	$+4.2 \times 10^{17}$	6.1×10^{-2}	p
ITO (100% Ar)	As-prepared	4.7×10^2	1.2×10^{-2}	-5.9×10^{19}	8.9×10^0	n
	Annealed	9.3×10^1	2.3×10^{-3}	-3.0×10^{20}	9.5×10^0	n

ITO films which were deposited followed the depositions of ZnO layers did not undergo any thermal treatment. The surface of the ITO films exhibited an rms roughness of around 2.7 nm which was slightly reduced to 2.3 nm after annealing as extracted from AFM observations (not shown here). The optical and electrical behavior of the as-prepared ITO films and their improvements after thermal treatment are presented in Fig. 2(c) and Table 1, respectively. Annealing of ITO improved crystallinity, healed defects, traps and structural imperfections leading to improved electrical characteristics like reduced resistivity, increased carrier concentration and a small increase of carriers' mobility. The improvement in the electrical properties of the ITO film after annealing was reflected in the reduced infra-red transmittance presented in Fig. 2(c) due to increased carrier concentration after annealing and thus increased carrier absorption. Similarly, the shift of the absorption edge to shorter wavelengths and thus increase of the energy band gap with annealing was due to the increase of carrier concentration and the Moss-Burstein effect [36].

In the next section the properties of the n/p ZnO homojunctions are presented where the diodes have the configuration: M2/n-ZnO/p-ZnO/M1/substrate, where the substrate can be glass or Si and M1, M2 can be metals or ITO. It is worth reminding that with the existing sputtering system and by performing the deposition on unintentionally heated substrates, the n-ZnO, p-ZnO and M2 layers could be deposited in a single deposition run without system venting and thus without exposing individual layers and interfaces to the detrimental effects of atmosphere exposure.

3.2. Characterization of the n/p ZnO diode

As shown in the previous section, all oxide layers fabricated in this investigation, n-ZnO, p-ZnO and ITO, were transparent and all of them could be grown on top of each other in a single growth run. The transparency of n/p ZnO homojunction was tested by fabricating the diode having the configuration ITO/n-ZnO/p-ZnO/ITO/glass and total thickness $d = 800$ nm. Fig. 3(a) shows the recorded

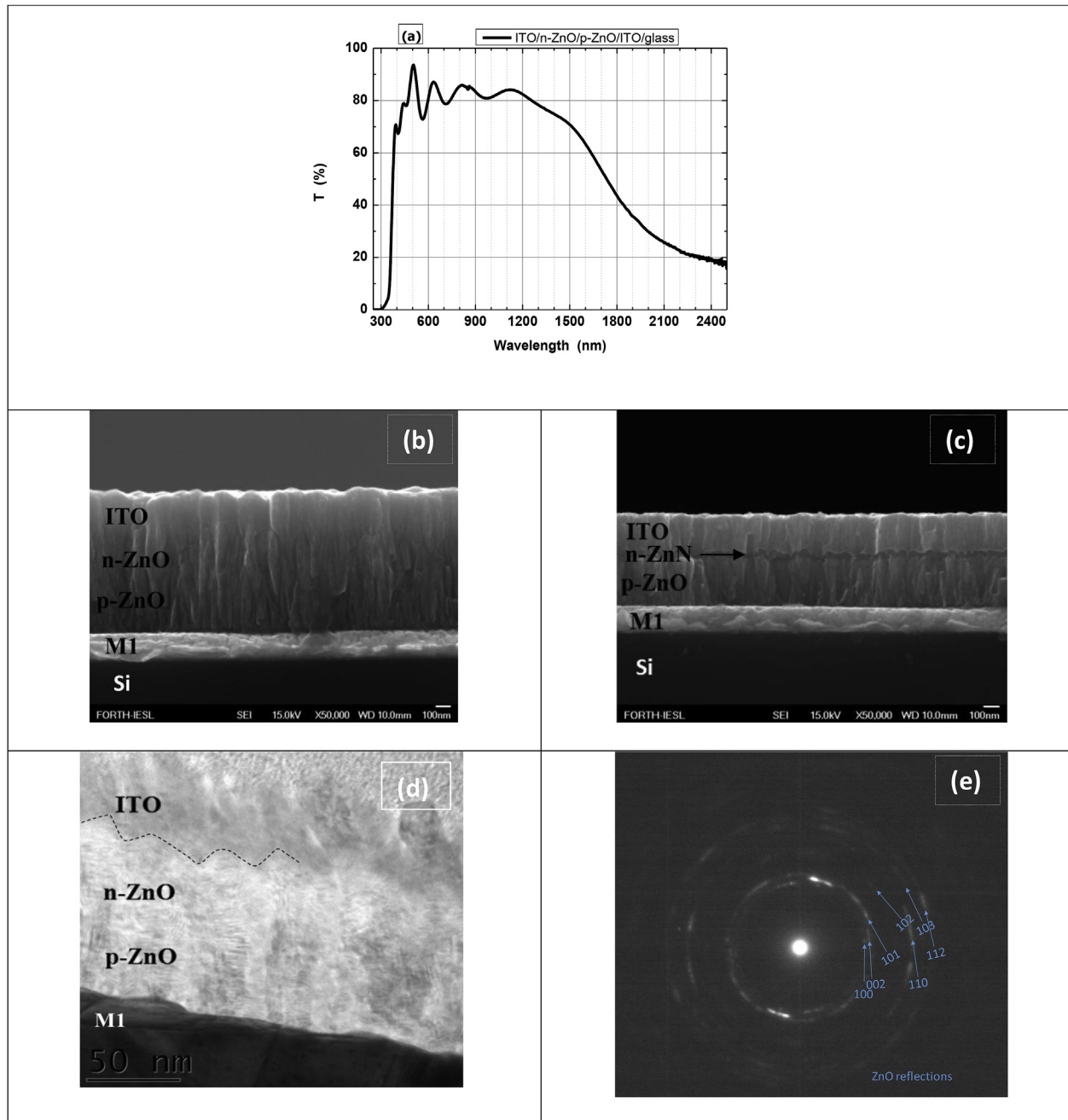


Fig. 3. (a) Transmittance of an n/p ZnO diode having the ITO/n-ZnO/p-ZnO/ITO/glass configuration, (b) cross-sectional SEM image of ITO/n-ZnO/p-ZnO/M1/Si diode, (c) cross-sectional SEM image of ITO/n-ZnN/p-ZnO/M1/Si diode, (d) XTEM image of ITO/n-ZnO/p-ZnO/M1/Si diode and (e) SAED pattern from the n/p ZnO seen in (d). M1: bottom metal contact.

transmittance (T) of the above multilayers. The n/p ZnO homo-junction sandwiched between two ITO layers and deposited on glass substrate had a visible transparency ($400\text{ nm} < \lambda < 700\text{ nm}$) of around 75–85%, it remained transparent at around 85% until the near infrared ($700\text{ nm} < \lambda < 1200\text{ nm}$) but the transmittance reduced for longer wavelengths due to increased absorption by carriers of the ITO-coated glass substrate (Fig. 2(c)).

To investigate the morphology of the structure by SEM and avoiding any charging effects, the ITO/glass substrate was replaced by metal-coated/Si (M1/Si) substrate and cross-sectional SEM image of the n/p ZnO homojunction having the ITO/n-ZnO/p-ZnO/M1/Si configuration is seen in Fig. 3(b). The structure of ZnO layers was

columnar, oriented perpendicular to the substrate. No interface can be distinguished between the p-ZnO and n-ZnO layers implying successful elimination of defects and extra states at the interface, whereas a clear interface can also be seen between the n-ZnO and ITO layers having different crystallographic phases (hexagonal n-ZnO and cubic ITO). For comparison reasons, the n-ZnO was replaced by a thin (around 50 nm) n-ZnN layer, made in 100% Ar plasma and having the cubic crystallographic phase [34], while keeping the deposition conditions of the p-ZnO layer the same like those of Fig. 3(b). The three distinct layers, p-ZnO, n-ZnN and ITO, can be clearly seen in the cross-sectional SEM images of Fig. 3(c). The columnar structure of a n/p ZnO homojunction, having a diode

thickness of around 130 nm, was examined by TEM and the results, XTEM image as well as spot reflections in SAED patterns, are depicted in Fig. 3(d) and (e). The growth mode of ZnO's grains and the lack of any interface imperfections between the p-ZnO and n-ZnO layers confirmed the observations made by the SEM images (Fig. 3(b)) that the n/p ZnO homojunction behaves crystallographically as a single phase wurtzite ZnO structure. This implies no discontinuities or states at the n-ZnO/p-ZnO interface indicating that any deterioration of the homojunction characteristics with time would arise mainly from the effects of its exposure to the atmosphere. The dash line has been drawn at the ZnO-ITO interface as a guide to the eye.

The electrical behavior of the n/p ZnO homojunction was tested after processing the structure as a diode having dot geometry employing the conventional substrate as well as the Si₃N₄-patterned substrate, as described in the Experimental Details section and illustrated in Fig. 1. After carefully examining and solving various processing issues encountered during diode fabrication the optimized patterned substrates were loaded into the sputtering chamber. The n/p ZnO diodes were grown on metal-coated glass substrates having the configuration M2/n-ZnO/p-ZnO/M1/glass where M1 was a Ag/Au metallization used as bottom contact to p-ZnO (Ag is acceptor for ZnO [7,37]) and M2 the Ti/Au top contact to n-ZnO. It is worth mentioning that the formation of ohmic contacts for p-ZnO and consequently for n/p ZnO homojunction is an open technological challenge not only because metals with high work functions are required but at the same time the difficulties in obtaining reliable p-ZnO layer and the associated stability issues of the layer have to be satisfied. It is not surprising that various metallization types have been reported in the literature, where single metals, bimetals or multilayer schemes have been applied as contacts to the p-ZnO and n-ZnO layers. Table 2 lists the metallization schemes for ZnO homojunctions reported over the last decade. In the present work, in order to avoid introducing any artifacts due to stability issues of the p-ZnO layer no tests were performed on the ohmic behavior of Ag/Au on p-ZnO. The Ti/Au metallization was used as ohmic contact for n-ZnO since it has been proven to be ohmic contact on n-ZnN layers (contact resistance $1.9 \times 10^{-4} \Omega \text{cm}^2$ [27]).

Fig. 4 shows the current–voltage (I–V) characteristics of the n/p ZnO homojunction diodes fabricated by the two different patterned substrates approach, seen in the inset, just after fabrication as well as after a period of five (5) months where the diodes had been left exposed to the ambient atmosphere. It was found that the I–V characteristics of the diodes showed rectifying behavior but the Si₃N₄-patterned diode (Fig. 4(b)) showed much more stable characteristics than the 'conventional' and unprotected diode (Fig. 4(a)). It should be reminded that the diode made on the Si₃N₄-patterned substrate was exposed to the ambient atmosphere only during

deposition of its top contact and during its 5 months exposure to the ambient was protected by the Si₃N₄ layer (see Fig. 1(b) and inset in Fig. 4(b)). The measured low current for the applied voltage might be due to high resistance of metal-semiconductor contacts, as mentioned above and the I–V hysteresis is associated with the trapping and detrapping of carriers in deep states within the structure during the I–V measurement. A turn on voltage (V_t) of around 1–1.5 V can be seen in Fig. 4(b) for the stable Si₃N₄-patterned homojunction. The build-in potential V_D of the diode was calculated from the equation [40]:

$$V_D = \frac{k_B T}{q} \left[\ln \frac{N_D N_A}{n_i^2} \right]$$

where $k_B T/q$ is the thermal voltage (25.58 meV), k_B is the Boltzmann constant, T is the room temperature 300 K, q is the electron charge, N_D and N_A are the donor concentration of n-ZnO ($1.6 \times 10^{18} \text{ cm}^{-3}$) and acceptor concentration of p-ZnO ($4.2 \times 10^{17} \text{ cm}^{-3}$), respectively (see Table 1), and n_i is the intrinsic carrier concentration of ZnO ($\sim 1 \times 10^6 \text{ cm}^{-3}$ [41]). The V_D value was found to be 1.20 eV which is in agreement with the turn-on voltage V_t of 1–1.5 V seen in the I–V curve of Fig. 4(b). Most of the reported values of V_t for ZnO homojunctions are generally observed between 1 and 3 V and differences between the values of V_D and V_t have been attributed to an increased resistance due to defects at the n-ZnO and p-ZnO interface introduced during the growth process [18]. Such imperfections at the interface have been eliminated in the n/p ZnO homojunction of this work where the transition from the p-ZnO to n-ZnO was done in a non-stop growth process. Stable ZnO homojunctions with low turn-on voltage values are two of the critical parameters for use in device applications. Additional work is needed to analyze further the I–V characteristics of the diode and tailor its properties, by applying the appropriate engineering procedures, in an effort to enhance output characteristics. Furthermore, it should be noted that the characterized n/p ZnO devices shown in Fig. 4 are not transparent since metallic contacts were used. However, as shown in the above sections, the presented results are very promising towards the fabrication of stable transparent all-oxide ZnO homodiodes in a rather facile way by applying the appropriate deposition and processing procedures. Moreover, the use of room temperature fabrication technique may promote them as potential candidates for flexible and wearable optoelectronic applications.

4. Conclusions

Concluding, a zinc nitride sputtering target was used to fabricate in a single growth run and at room temperature transparent and stable n/p ZnO homojunction thin film structures. The bipolar N-containing ZnO layers were successively deposited by adjusting the

Table 2
Reported metallization schemes, over the last decade, as contacts for ZnO homojunctions.

n-ZnO ohmic contact	p-ZnO ohmic contact	[Ref.] Year
Au	Au	[11] 2017, [17] 2013
In	In	[21] 2014, [20] 2013, [19] 2012, [9] 2011
Pt	Pt	[15] 2017
silver-paste	silver-paste	[10] 2012
In	Ni/Au	[12] 2013
In/Au	In/Au	[14] 2008
In/Zn	In/Zn	[16] 2008
Zn:Al	Zn:Al	[25] 2013
Ti/Au	Ti/Au	[24] 2015
Ti/Au	Ag/Au	Present Work
Ti/Au	ITO	[38] 2011
ITO-ZnO	Ni/Au	[39] 2015

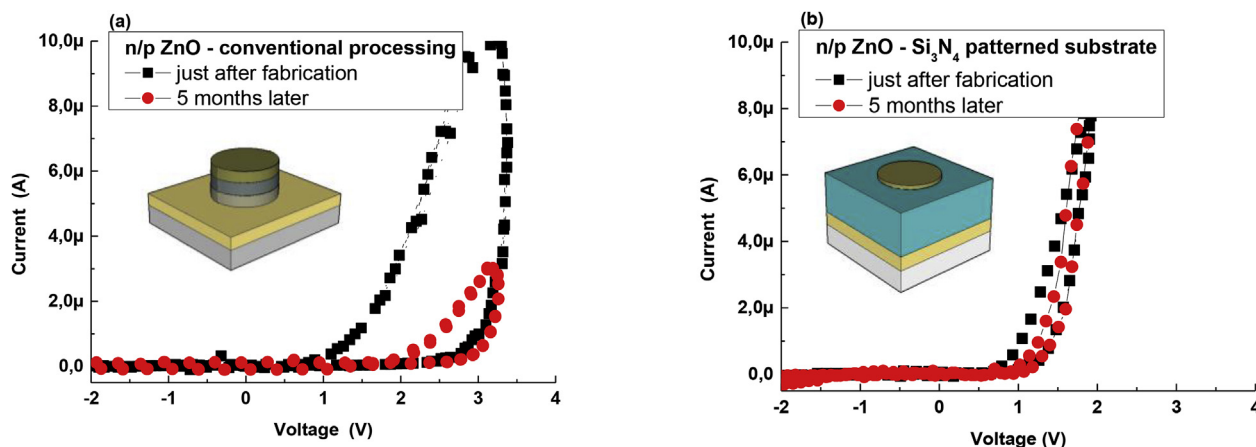


Fig. 4. I-V characteristics of n/p ZnO homojunctions processed (a) 'conventional' non-patterned substrate and (b) on Si_3N_4 -patterned substrate just after fabrication and after five (5) months. The inset shows schematic representations of the diodes, the cross-section of which are seen Fig. 1.

O_2 content of the O_2 -Ar plasma through mass flow controllers for transforming from the n-type ZnO to p-type ZnO layers. N-type ZnO was formed in low- O_2 plasma (10% O_2) whereas O_2 -rich plasma formed p-type ZnO layer. The transparency of the homojunction was tested having the all-oxide configuration ITO/n-ZnO/p-ZnO/ITO/glass, made without breaking sputtering vacuum during depositions thus eliminating any imperfections at the layers' interfaces. The transmittance was found to be around 75–85% in the visible solar spectrum region. The stability of ZnO homojunction was examined by forming the n/p ZnO configuration metal/n-ZnO/p-ZnO/metal/Si on conventionally processed Si substrate and on Si substrate coated by a patterned Si_3N_4 layer. The Si_3N_4 layer played the role of protective layer for the ZnO homojunction as a result of which exposing the diodes to the ambient atmosphere for five months provided stable I–V characteristics when compared to the diode formed on conventional substrates. With a turn-on voltage of around 1.5 V and by further optimizing the layers properties as well as the processing procedure steps, ZnO homojunctions with enhanced diode characteristics and stability may be realized for flexible and wearable optoelectronic devices applications.

Acknowledgements

This work was partially supported by the EU Horizon 2020 'ASCENT' project, grant agreement No 654384 (project 046), the "Materials and Processes for Energy and Environment Applications-AENAO" (MIS 5002556) project co-financed by Greece and EU (European Regional Development Fund), the EU's FP7/2007–2013 project "Oxide Materials Towards a Matured Post-silicon Electronics Era -ORAMA" (contract no. NMP3-LA-2010-246334) and the project "Electronics Beyond Silicon Era" (ELBESIER) Erasmus+ KA2 programme.

References

- [1] Yun J. Ultrathin metal films for transparent electrodes of flexible optoelectronic devices. *Adv Funct Mater* 2017;27(1–21):1606641. <https://doi.org/10.1002/adfm.201606641>.
- [2] Zhan Z, An J, Wei Y, Tran VT, Du H. Inkjet-printed optoelectronics. *Nanoscale* 2017;9:965–93. <https://doi.org/10.1039/C6NR08220C>.
- [3] Gagaoudakis E, Michail G, Aperathitis E, Kortidis I, Binas V, Panagopoulou M, Raptis YS, Tsoukalas D, Kiriakidis G. Low temperature rf-sputtered thermochromic VO_2 films on flexible glass substrates. *Adv Mat Lett* 2017;8:757–61. <https://doi.org/10.5185/amlett.2017.6934>.
- [4] Cai G, Wang J, Lee PS. Next-generation multifunctional electrochromic devices. *Acc Chem Res* 2016;49:1469–76. <https://doi.org/10.1021/acs.accounts.6b00183>.
- [5] Iseri E, Kuzum D. Implantable optoelectronic probes for in vivo optogenetics. *J Neural Eng* 2017;14(1–18):031001. <https://doi.org/10.1088/1741-2552/aa60b3>.
- [6] Tang K, Gu S-L, Ye J-D, Zhu S-M, Zhang R, Zheng Y-D. Recent progress of the native defects and p-type doping of zinc oxide. *Chin Phys B* 2017;26(1–23):047702. <https://doi.org/10.1088/1674-1056/26/4/047702>.
- [7] Grundmann M, Klüpfel F, Karsthorst R, Schlupp P, Schein F-L, Splith D, Yang C, Bitter S, von Wenckstern H. Oxide bipolar electronics: materials, devices and circuits. *J Phys D: Appl Phys* 2016;49(25pp):213001. <https://doi.org/10.1088/0022-3727/49/21/213001>.
- [8] Xiong G, Wilkinson J, Mischuck B, Tuzemen S, Ucer KB, Williams RT. Control of p- and n-type conductivity in sputter deposition of undoped ZnO. *Appl Phys Lett* 2002;80:1195–7. <https://doi.org/10.1063/1.1449528>.
- [9] Balakrishnan L, Premchander P, Balasubramanian T, Gopalakrishnan N. Al-N codoping and fabrication of ZnO homojunction by RF sputtering. *Vacuum* 2011;85:881–6. <https://doi.org/10.1016/j.vacuum.2011.01.003>.
- [10] Dhara S, Giri PK. Stable p-type conductivity and enhanced photoconductivity from nitrogen-doped annealed ZnO thin film. *Thin Solid Films* 2012;520:5000–6. <https://doi.org/10.1016/j.tsf.2012.02.081>.
- [11] Rakhshani AE. Characterization and device applications of p-type ZnO films prepared by thermal oxidation of sputter-deposited zinc oxynitride. *J Alloy Comp* 2017;695:124–32. <https://doi.org/10.1016/j.jallcom.2016.10.187>.
- [12] Sui YR, Yao B, Xiao L, Yang LL, Cao J, Li XF, Xing GZ, Lang JH, Li XY, Lv SQ, Meng XW, Liu XY, Yang JH. Fabrication and characterization of P–N dual acceptor doped p-type ZnO thin films. *Appl Surf Sci* 2013;287:484–9. <https://doi.org/10.1016/j.apsusc.2013.10.010>.
- [13] Tsukazaki A, Ohtomo A, Onuma T, Ohtani M, Makino T, Sumiya M, Ohtani K, Chichibu SF, Fuke S, Segawa Y, Ohno H, Koinuma H, Kawasaki M. Repeated temperature modulation epitaxy for p-type doping and light-emitting diode based on ZnO. *Nat Mater* 2005;4:42–6. <https://doi.org/10.1038/nmat1284>.
- [14] Lu JG, Fujita S, Kawaharamura T, Nishinaka H, Kamada Y. Junction properties of nitrogen-doped ZnO thin films. *Phys Status Solidi C* 2008;5:3088–90. <https://doi.org/10.1002/pssc.200779171>.
- [15] Wang Y, Chen Y, Zhao W, Ding L, Wen L, Li H, Jiang F, Su J, Li L, Liu N, Gao Y. A self-powered fast-response ultraviolet detector of p–n homojunction assembled from two ZnO-based nanowires. *Nano-Micro Lett* 2017;9(1–7):11. <https://doi.org/10.1007/s40820-016-0112-6>.
- [16] Lin SS, Lu JG, Ye ZZ, He HP, Gu XQ, Chen LX, Huang JY, Zhao BH. p-type behavior in Na-doped ZnO films and ZnO homojunction light-emitting diodes. *Solid State Commun* 2008;148:25–8. <https://doi.org/10.1016/j.ssc.2008.07.028>.
- [17] Yu S, Ding L, Zheng H, Xue C, Chen L, Zhang W. Electrical and photoelectric properties of transparent Li-doped ZnO/ZnO homojunctions by pulsed laser deposition. *Thin Solid Films* 2013;540:146–9. <https://doi.org/10.1016/j.tsf.2013.05.125>.
- [18] Yang X, Xu X, Liu F, Zhang L, Ji Z, Chen Q, Cao B. Fabrication of p-ZnO:Na/n-ZnO:Na homojunction by surface pulsed laser irradiation. *RSC Adv* 2017;7:37296–301. <https://doi.org/10.1039/c7ra05574a>.
- [19] Yang T-H, Wu J-M. Thermal stability of sol–gel p-type Al–N codoped ZnO films and electric properties of nanostructured ZnO homojunctions fabricated by spin-coating them on ZnO nanorods. *Acta Mater* 2012;60:3310–20. <https://doi.org/10.1016/j.actamat.2012.02.045>.
- [20] Swapna R, Kumar MCS. Deposition of Na–N dual acceptor doped p-type ZnO thin films and fabrication of p-ZnO:(Na,N)/n-ZnO:Eu homojunction. *Mater Sci Eng B* 2013;178:1032–9. <https://doi.org/10.1016/j.mseb.2013.06.010>.
- [21] Swapna R, Kumar MCS. Fabrication and characterization of n-ZnO:Eu/p-ZnO:(Ag,N) homojunction by spray pyrolysis. *Mater Res Bull* 2014;49:44–9. <https://doi.org/10.1016/j.materresbull.2013.08.045>.

- [22] Bian JM, Li XM, Zhang CY, Yu WD, Gao XD. p-type ZnO films by monodoping of nitrogen and ZnO-based homojunctions. *Appl Phys Lett* 2004;85:4070–2. <https://doi.org/10.1063/1.1808229>.
- [23] Bian JM, Li XM, Zhang CY, Chen LD, Yao Q. Synthesis and characterization of two-layer-structured ZnO homojunctions by ultrasonic spray pyrolysis. *Appl Phys Lett* 2004;84:3783–5. <https://doi.org/10.1063/1.1739280>.
- [24] Snigurenko D, Kopalko K, Krajewski TA, Jakiela R, Guziewicz E. Nitrogen doped p-type ZnO films and p-n homojunction. *Semicond Sci Technol* 2015;30:1–6. <https://doi.org/10.1088/0268-1242/30/1/015001>. 015001.
- [25] Bu IYY. Room temperature deposition of graded ZnO homojunction from a single sputter target. *Superlattice Microst* 2013;64:213–9. <https://doi.org/10.1016/j.spmi.2013.08.018>.
- [26] Wei ZP, Lu YM, Shen DZ, Zhang ZZ, Yao B, Li BH, Zhang JY, Zhao DX, Fan XW, Tang ZK. Room temperature ZnO blue-violet light-emitting diodes. *Appl Phys Lett* 2007;90(1–3):042113. <https://doi.org/10.1063/1.2435699>.
- [27] Kambilafka V, Kostopoulos A, Androulidaki M, Tsagaraki K, Modreanu M, Aperathitis E. Transparent p/n diode device from a single zinc nitride sputtering target. *Thin Solid Films* 2011;520:1202–6. <https://doi.org/10.1016/j.tsf.2011.06.072>.
- [28] Stroescu H, Anastasescu M, Preda S, Nicolescu M, Stoica M, Stefan N, Kampylafka V, Aperathitis E, Modreanu M, Zaharescu M, Gartner M. Influence of thermal treatment in N₂ atmosphere on chemical, microstructural and optical properties of indium tin oxide and nitrogen doped indium tin oxide rf-sputtered thin films. *Thin Solid Films* 2013;541:121–6. <https://doi.org/10.1016/j.tsf.2012.11.135>.
- [29] Nicolescu M, Anastasescu M, Preda S, Calderon-Moreno JM, Osiceanu P, Gartner M, Teodorescu VS, Maraloiu AV, Kampylafka V, Aperathitis E, Modreanu M. Investigation of microstructural properties of nitrogen doped ZnO thin films formed by magnetron sputtering on silicon substrate. *J Optoelectron Adv Mater* 2010;12:1045–51.
- [30] Liang HW, Lu YM, Shen DZ, Yan JF, Li BH, Zhang JY, Liu YC, Fan XW. Investigation of growth mode in ZnO thin films prepared at different temperature by plasma-molecular beam epitaxy. *J Cryst Growth* 2005;278:305. <https://doi.org/10.1016/j.jcrysgro.2005.01.024>.
- [31] Zeng YJ, Ye ZZ, Xu WZ, Lu JG, He HP, Zhu LP, Zhao BH, Che Y, Zhang SB. p-type behavior in nominally undoped ZnO thin films by oxygen plasma growth. *Appl Phys Lett* 2006;88:262103. <https://doi.org/10.1063/1.2217165>.
- [32] Lu J, Liang Q, Zhang Y, Ye Z, Fujita S. Improved p-type conductivity and acceptor states in N-doped ZnO thin films. *J Phys D: Appl Phys* 2007;40:3177. <https://doi.org/10.1016/j.tsf.2014.02.109>.
- [33] Nicolescu M, Anastasescu M, Preda S, Calderon-Moreno JM, Stroescu H, Gartner M, Teodorescu VS, Maraloiu AV, Kampylafka V, Aperathitis E, Modreanu M. Surface topography and optical properties of nitrogen doped ZnO thin films formed by radio frequency magnetron sputtering on fused silica substrates. *J Optoelectron Adv Mater* 2010;12:1343–9.
- [34] Voulgaropoulou P, Dounis S, Kambilafka V, Androulidaki M, Ruzinsky M, Sály V, Prokein P, Viskadourakis Z, Tsagaraki K, Aperathitis E. Optical properties of zinc nitride thin films fabricated by rf-sputtering from ZnN target. *Thin Solid Films* 2008;516:8170–4. <https://doi.org/10.1016/j.tsf.2008.04.025>.
- [35] Kim IY, Shin SW, Gang MG, Lee SH, Gurav KV, Patil PS, Yun JH, Lee JY, Kim JH. Comparative study of quaternary Mg and Group III element co-doped ZnO thin films with transparent conductive characteristics. *Thin Solid Films* 2014;570:321–5. <https://doi.org/10.1016/j.tsf.2014.02.109>.
- [36] Hamberg I, Granqvist CG, Berggren K-F, Sernelius BE, Engstrom L. Band-gap widening in heavily Sn-doped In₂O₃. *Phys RevB* 1984;30:3240–9.
- [37] Fan JC, Sreekanth KM, Xie Z, Chang SL, Rao KV. p-Type ZnO materials: theory, growth, properties and devices. *Prog Mater Sci* 2013;58:874–985. <https://doi.org/10.1016/j.pmatsci.2013.03.002>.
- [38] Wang G, Chu S, Zhan N, Lin Y, Chernyak L, Liu J. ZnO homojunction photodiodes based on Sb-doped p-type nanowire array and n-type film for ultra-violet detection. *Appl Phys Lett* 2011;41107:1–3. <https://doi.org/10.1063/1.3551628>.
- [39] Chiu H-J, Chen T-H, Lai L-W, Lee C-T, Hong J-D, Liu D-S. The achievement of a zinc oxide-based homojunction diode using radio frequency magnetron cosputtering system. *J Nanomater* 2015. <https://doi.org/10.1155/2015/284835>. Article ID 284835, 8 pages.
- [40] Sze SM. In: *Semiconductor devices: physics and technology*. J. Wiley & Sons; 1985. p. 70. ISBN: 0-471-87424-8, chap. 3.
- [41] Norton DP, Heo YW, Ivill MP, Ip K, Pearton SJ, Chisholm MF, Steiner T. ZnO: growth, doping & processing. *Mater Today* 2004;7:34–40.



Dr. ELIAS APERATHITIS: Physicist- Application Scientist, at the Microelectronics Research Group (MRG) of IESL/FORTH in Crete, Greece. He received his M.Sc. from Univ. of Dundee, Scotland and his Ph.D. from Hull Univ., England. He has conducted research in the fabrication/processing and characterization of compound semiconductors (III–V, III–N & oxides) materials/devices and he is currently involved in the development of novel thin film oxide/nitride/oxynitride-based materials and devices for transparent micro-nano-electronics, optoelectronics and energy efficient buildings.